World Journal of Microbiology and Biotechnology (2020) 36:174
https://doi.org/10.1007/s11274-020-02948-6

ORIGINAL PAPER

Anti-Staphylococcal and cytotoxic activities of the short anti-microbial peptide PVP

Hamed Memariani[1] · Mojtaba Memariani[1] · Reza Mahmoud Robati[1,2] · Soheila Nasiri[1,2] · Fahimeh Abdollahimajd[1] · Zohre Baseri[3] · Hamideh Moravvej[1]

Received: 23 June 2020 / Accepted: 8 October 2020 / Published online: 21 October 2020

Abstract

Over the past years, short anti-microbial peptides have drawn growing attention in the research and trade literature because they are usually capable of killing a broad spectrum of pathogens by employing unique mechanisms of action. This study aimed to evaluate the anti-bacterial effects of a previously designed peptide named PVP towards the clinical strains of methicillin-resistant *Staphylococcus aureus* (MRSA) in vitro. Secondary structure, cytotoxicity, and membrane-permeabilizing effects of the peptide were also assessed. PVP had a tendency to adopt alpha-helical conformation based upon structural predictions and circular dichroism spectroscopy (in 50% trifluoroethanol). The peptide showed MIC values ranging from 1 to 16 µg/mL against 10 strains of MRSA. In contrast to ciprofloxacin and gentamicin, PVP at sub-lethal concentration (1 µg/mL) did not provoke the development of peptide resistance after 14 serial passages. Remarkably, 1 h of exposure to 4 × MBC of PVP (8 µg/mL) was sufficient for total bacterial clearance, whereas 4 × MBC of vancomycin (8 µg/mL) failed to totally eradicate bacterial cells, even after 8 h. PVP showed negligible cytotoxicity against human dermal fibroblasts at concentrations required to kill the MRSA strains. The results of flow cytometric analysis and fluorescence microscopy revealed that PVP caused bacterial membrane permeabilization, eventually culminating in cell death. Owing to the potent anti-bacterial activity, fast bactericidal kinetics, and negligible cytotoxicity, PVP has the potential to be used as a candidate antibiotic for the topical treatment of MRSA infections.

Keywords Anti-microbial peptide · Methicillin-resistant *Staphylococcus aureus* · Bactericidal activity · Human dermal fibroblasts · Membrane permeabilization

Abbreviations

AMPs	Anti-microbial peptides
AO/EtBr	Acridine orange/ethidium bromide
CD	Circular dichroism
CFUs	Colony forming units
DMEM	Dulbecco's Modified Eagle's Medium
HDFs	Human dermal fibroblasts
MBC	Minimum bactericidal concentration
MDR	Multidrug resistant
MHB	Müeller-Hinton broth
MIC	Minimum inhibitory concentration
MRSA	Methicillin-resistant *Staphylococcus aureus*
PBS	Phosphate-buffered saline
PCR	Polymerase chain reaction
PI	Propidium iodide
RP-HPLC	Reversed-phase high performance liquid chromatography
SI	Selectivity index
SD	Standard deviation
TFE	Trifluoroethanol
TSB	Tryptic soy broth

✉ Mojtaba Memariani
memaryani@gmail.com

✉ Hamideh Moravvej
hamidehmoravej@sbmu.ac.ir

[1] Skin Research Center, Shahid Beheshti University of Medical Sciences, Tehran, Iran

[2] Department of Dermatology, Loghman Hakim Hospital, Shahid Beheshti University of Medical Sciences, Tehran, Iran

[3] Department of Pathology and Laboratory Medicine, Shariati Hospital, Tehran University of Medical Sciences, Tehran, Iran

Introduction

The indiscriminate and injudicious use of antibiotics for treating infectious diseases has led to the emergence of multidrug-resistant (MDR) bacterial pathogens, accelerating the obsolescence of the available antibiotics (Hotchkiss and Opal 2020). In particular, ESKAPE pathogens (i.e. *Enterococcus faecium*, *Staphylococcus aureus*, *Klebsiella pneumoniae*, *Acinetobacter baumannii*, *Pseudomonas aeruginosa*, and *Enterobacter* species) are regarded as a major public health threat due to their capability of developing resistance to traditional anti-microbial therapies (Reuter and Kruger 2020). In this respect, *S. aureus* can cause a broad spectrum of illnesses, ranging from mild skin infections to serious and life-menacing diseases. MRSA was first isolated in the early 1960s, immediately after methicillin came into use as an antibiotic. In some reports, MRSA comprises more than half of all clinical *S. aureus* strains (Morelli et al. 2015; Chatterjee et al. 2018). The pathogen still remains as a great concern in both community and hospital settings owing to the fact that it can readily become resistant to multiple classes of antibiotics (especially aminoglycosides and glycopeptides), thereby limiting the treatment options (Kluytmans and Harbarth 2020). In Europe, around 5,400 deaths as well as over a million extra days of hospitalization due to MRSA are estimated to occur each year (Gould et al. 2012). In the United States, more than 323,000 hospitalized patients were infected with MRSA in 2017, of whom nearly 10,600 succumbed to death (CDC 2019). This deplorable situation of antibiotic resistance necessitates urgent actions to discover and develop novel classes of anti-microbials with low predilection for microbial drug resistance.

Anti-microbial peptides (AMPs), also dubbed host defense peptides, are evolutionarily crafted multipotent molecules of innate immune systems in the living creatures (Brand et al. 2019). Most AMPs exert inhibitory or killing effects on bacteria, fungi, protozoans, and viruses (Shagaghi et al. 2018; Memariani and Memariani 2020a). Aside from documented anti-microbial features, these intriguing peptides may exert a wide array of biological functions such as anti-tumor, anti-inflammatory, anti-biofilm, lipopolysaccharide-neutralizing, and adjuvant activities. Regardless of a perplexing diversity in their primary sequences, AMPs typically encompass 12 to 50 amino acid residues with an amphipathic nature and a net positive charge at physiological pH (Haney et al. 2019). On the basis of their secondary structure, they are categorized into four classes, namely α-helical, β-sheet, extended, and loop peptides. Natural or synthetically designed, the majority of AMPs are believed to attack microorganisms through a receptor-independent mediated membrane permeabilization, though some act on intracellular targets including DNA, RNA, and enzymes (Wibowo and Zhao 2019). It is generally now accepted that most AMPs kill bacteria in a relatively short time by employing unique mechanisms of action which are distinct from those of conventional antibiotics. Thus, they are less prone to invoke microbial drug resistance (Moravvej et al. 2020). Moreover, there is a voluminous body of literature regarding synergisms between AMPs and antibiotics against both the planktonic and biofilm-residing bacteria (Lazzaro et al. 2020; Zhang et al. 2014).

While AMPs hold promise in filling the antibiotic discovery void, several obstacles including host cell toxicity, high production costs, and low stability still lie ahead for their development as therapeutically applicable anti-microbials. To triumph over these constraints, various strategies have been employed such as natural and unnatural amino acid residual replacement, N- and C-terminal modifications, truncation, cyclization, dimerization, hybridization, and nano-encapsulation, to mention just a few (Ong et al. 2014). In particular, hybridizing different fragments of AMPs to construct novel hybrids has attracted the researchers' attention because hybrid AMPs can embody higher therapeutic indices compared with their parental counterparts (Wang et al. 2019).

Over the last decades, short AMPs (< 20 amino acid residues) devoid of disulfide bonds have begun to garner plenty of attention in the academia and commercial spheres for either prophylaxis or treatment of various infections, particularly those caused by dermatologically relevant pathogens (Mikut et al. 2016; Mishra et al. 2017; Rahnamaeian and Vilcinskas 2015). For instance, several short AMPs are in clinical trials or preclinical development for topical treatment of skin diseases such as MRSA skin infections, impetigo, fungal nail infections, and acne rosacea (Mookherjee et al. 2020; Koo and Seo 2019). The absence of disulfide bonds in peptide structures obviates the need for supplementary folding steps, which would reduce costs of large-scale production (Rahnamaeian and Vilcinskas 2015). Besides this, short AMPs are less likely to evoke inapt immune responses (Mikut et al. 2016).

In our earlier study, we assessed a series of short hybrid peptides lacking disulfide bonds which were designed based upon three naturally occurring AMPs (pEM-2, mastoparan-VT1, and mastoparan-B) from animal venoms (Memariani et al. 2017). Among designed hybrids, peptides PV3 and PVP displayed higher anti-bacterial activities and lower hemolysis rates as compared with their parental peptides. This study aimed to appraise anti-bacterial properties of the synthetic hybrid peptide PVP towards the clinical strains of MRSA. We have also evaluated secondary structure, cytotoxicity, and membrane-permeabilizing effects of the hybrid peptide.

Materials and methods

Reagents and media

All the common chemical reagents employed in the present study were of analytical grade from commercial suppliers. Trifluoroethanol (TFE), Müeller-Hinton broth (MHB), tryptic soy broth (TSB), and agar-agar were procured from Merck Co. (Darmstadt, Germany), while flat-bottom 96-well polystyrene plates were obtained from SPL Life Science Co. (Gyeonggi-do, Republic of Korea). Furthermore, antibiotics were purchased from Oxoid Ltd. (Basingstoke, Hampshire, UK). The other materials were all supplied by Sigma–Aldrich Chemical Co. (St. Louis, MO, USA).

Peptide analysis and synthesis

The secondary and tertiary structures of PVP (KKWRKLLKWLAKK) were predicted by SABLE Protein prediction (https://sable.cchmc.org) and I-TASSER (http://zhanglab.ccmb.med.umich.edu/I-TASSER/) servers, respectively. Furthermore, helical wheel diagram of the peptide was created as described by Schiffer and Edmundson (1967).

PVP was synthesized with carboxyl-amidated C-terminus under good manufacturing practice regulations by a multistep solid-phase technique using N-9-fluorenylmethoxycarbonyl (Fmoc) chemistry (Smart et al. 1996). The purity of the synthetic peptide was evaluated using reversed-phase high performance liquid chromatography (RP-HPLC). Moreover, the identity of PVP was confirmed by mass spectrometry on a Sciex API100 LC/MS instrument (PerkinElmer Co., Norwalk, CT, USA) in positive ion mode. The lyophilized peptide was aseptically dissolved in double-distilled water (final stock concentration of 1.28 mg/mL) and stored at − 80 °C until further use.

Secondary structure analysis of the peptide

Circular dichroism (CD) spectra were routinely recorded at 25 °C on an AVIV MODEL 215 spectropolarimeter (AVIV Instruments, Inc., Lakewood, NJ, USA) equipped with a 0.1-cm path-length cell (Hellma, Forest Hills, NY, USA) to delineate secondary structures of PVP in different environments (Memariani et al. 2018). For this purpose, peptide solutions (at a final concentration of 0.2 mg/mL) were prepared in deionized water either in the presence or absence of 50% (*v*/*v*) TFE. TFE acts as a membrane-mimicking environment. Several scans between a wavelength range of 190 and 260 nm with the scanning speed of 20 $nm.min^{-1}$ were averaged and corrected for background scattering through subtraction of respective blank runs from the appropriate spectra of PVP. The mean residue molar ellipticity ($[\theta]$) was calculated by the following equation:

$$[\theta] = \frac{\theta}{10 \times l \times c_M \times n}$$

Where θ, l, c_M, and n are the ellipticity, the optical path length of the cell, the peptide concentration, and the number of amino acid residues in the peptide, respectively (Lee et al. 2003).

Furthermore, CDNN 2.0 software (Gerald Böhm, Martin-Luther-Universität Halle-Wittenberg, Germany) was used in order to quantify secondary structure contents of the peptide.

Bacterial strains and culture conditions

Ten clinical strains of *S. aureus* (Table 1) were included in this study. These strains were confirmed to be *S. aureus* using established methods, including colonial appearance, Gram stain characteristics, the existence of catalase activity, and capability of coagulating rabbit serum (Tille 2017).

Given that results of cefoxitin disk diffusion testing (30 µg) are easier to interpret and are thus more susceptible for the detection of methicillin resistance than oxacillin results, we used the former method for phenotypic detection of MRSA

Table 1 Characterization of MRSA strains isolated from patients during November 2018 through January 2020

Isolate ID	Specimen site	Date of isolation (month/year)	Characterization of patients		*mec A* gene
			Age	Gender	
AS1	Ascitic fluid	12/2019	38	M	+
B1	Blood	01/2020	72	F	+
B2	Blood	01/2020	48	F	+
WT1	Wound or tissue	11/2018	51	F	+
WT2	Wound or tissue	12/2018	20	M	+
WT3	Wound or tissue	03/2019	82	F	+
WT4	Wound or tissue	03/2019	64	M	-
WT5	Wound or tissue	05/2019	16	M	+
WT6	Wound or tissue	06/2019	63	M	+
WT7	Wound or tissue	08/2019	54	M	+

strains (Boutiba-Ben Boubaker et al. 2004). This was further confirmed by polymerase chain reaction (PCR) detection of *mecA* gene using specific primers MEC1 (5′-AAAATCGATGGTAAAGGTTGGC-3′) and MEC2 (5′-AGTTCTGCAGTACCGCATTTGC-3′), as described elsewhere (Murakami et al. 1991). *S. aureus* ATCC 700699 and ATCC 29213 were also used as positive and negative controls, respectively.

The aforementioned strains were then stored frozen at − 80 °C in TSB supplemented with 20% (*v*/*v*) glycerol. Bacterial strains to be tested were revived from frozen glycerol stocks, sub-cultured twice on trypticase soy agar containing 5% sheep erythrocyte, and incubated aerobically at 37 °C for up to 18 h in order to provide fresh colonies. One strain of MRSA (WT1) was also selected for multistep resistance selection assay, kinetics of bacterial killing, fluorescence microscopy, and flow cytometric analysis.

In vitro anti-bacterial assays

Minimum inhibitory concentration (MIC) values of PVP and antibiotics including oxacillin and vancomycin for each isolate were appraised using broth microdilution method in accordance with guidelines promulgated by Clinical and Laboratory Standards Institute (CLSI 2019). In brief, exponentially growing bacteria were harvested, re-suspended in MHB to yield 5×10^5 CFUs/mL, and added to 96-well plates containing two-fold serially diluted anti-bacterial agents. The final concentrations of the anti-bacterial agents ranged from 0.25 to 128 µg/mL. Following 20 h of incubation at 37 °C, bacterial growth was determined by quantifying the optical density at 600 nm using a microplate spectrophotometer (Bio-Rad 680, CA, USA). Wells devoid of the peptide and bacteria were served as positive and negative controls, respectively. MIC was regarded as the lowest anti-microbial concentration at which there was no evidence of bacterial growth.

From the clear wells, 10 µL of broth was removed and streaked onto Müeller-Hinton agar plates. Shortly afterwards, the plates were incubated at 37 °C for 24 h. Minimum bactericidal concentration (MBC) was determined as the lowest anti-microbial concentration at which a reduction of 99.9% in CFUs was detected (Memariani et al. 2018).

Determination of anti-bacterial activity index

Anti-bacterial capacity of the peptide and antibiotics against each strain can be calculated as the quotient of the MBC and the MIC (Konaté et al. 2012):

$$\text{Anti-bacterial activity index} = \frac{\text{MBC}}{\text{MIC}}$$

The anti-bacterial activity index was interpreted as follows: Bactericidal activity: MBC/MIC ≤ 2, bacteriostatic activity: 4 ≤ MBC/MIC < 32, and tolerance: MBC/MIC ≥ 32.

Multistep resistance selection assay

To shed some light on the possibility of bacterial resistance selection (MRSA WT1) under pressure of PVP, ciprofloxacin, and gentamicin in vitro, multistep resistance selection assay was performed. Drug resistant development of MRSA WT1 was monitored daily upon treating bacterial cells repeatedly with 0.5 × MIC of anti-bacterial agents by calculating fold-change in MIC (Wiradharma et al. 2011a):

$$\text{Fold-change in MIC} = \frac{\text{MIC}_n}{\text{MIC}_1}$$

Where MIC_n and MIC_1 represent the MIC value at passage *n* and the initial MIC value, respectively. The initial MIC values for PVP, ciprofloxacin, and gentamicin were 2, 1, and 2 µg/mL, respectively.

Kinetics of bacterial killing

The rates at which anti-bacterial agents can kill bacteria were determined by incubating 5×10^5 CFUs/mL of MRSA with 1×, 2×, and 4 × MBC of PVP and vancomycin individually at 37 °C for various durations. At specified time points, aliquots of each sample were taken, serially diluted in phosphate-buffered saline (PBS), and plated onto Müeller-Hinton agar plates (Guinoiseau et al. 2010). Finally, CFUs were counted after 20 h of incubation at 37 °C.

Bacterial viability assay

Acridine orange/ethidium bromide (AO/EtBr) double staining method followed by fluorescence microscopy (Baskić et al. 2006) was adopted to gain further clues concerning bactericidal effects of PVP. Briefly, bacterial cell suspensions (~ 10^7 CFUs/mL) were incubated with 1 × and 2 × MBC of PVP or vancomycin separately at 37 °C for 1 h. Afterwards, 50 µL of bacterial cell suspension was mixed with 10 µL of dye mixture (100 µg/mL AO and 100 µg/mL EtBr in distilled water) on a clean microscope slide, and then immediately visualized using fluorescence microscopy (Zeiss, Oberkochen, Germany). The data were analyzed using Axiovision 4.8 software (Carl Zeiss, Germany). Fluorescence images were also processed using ImageJ software (NIH, rsb.info.nih.gov/ij/) in order to calculate the percentage of surface area covered by stained bacteria.

Membrane permeabilization assay

In order to elucidate whether PVP can provoke membrane permeabilization, a flow cytometric analysis based on propidium iodide (PI) was performed, as described elsewhere

(Jeyanthi and Velusamy 2016). In brief, MRSA cells were grown in MHB to a mid-logarithmic phase, washed thrice in PBS, adjusted to 5×10^5 CFUs/mL in the same buffer, and incubated with PVP (1 × and 2 × MBC) and vancomycin (1 × and 2 × MBC) individually at 37 °C for 1 h. These bacterial cells were then incubated with PI (at a final concentration of 2 µg/mL) for 15 min to permit the dye uptake, prior to recording fluorescence intensities by a FACSCalibur flow cytometer (Becton Dickinson Biosciences, CA, USA). Peptide-treated samples were also compared to the negative control (PBS-treated) using CellQuest Pro software version 5.1 (BD Biosciences).

Isolation and culture of fibroblasts

Human dermal fibroblasts (HDFs) were retrieved from the foreskin of a male infant without known dermatological or genetic diseases (Moravvej et al. 2018). To this end, the foreskin tissue was stored overnight at 4 °C in Dulbecco's Modified Eagle's Medium (DMEM) containing 10% (*v*/*v*) antibiotic–antimycotic solution, washed thrice in PBS, minced into small pieces, and incubated with Dispase at 4 °C for 16 h. Skin dermis was gently separated from the epidermis using two pairs of curved forceps, chopped into very small pieces, and incubated in type I collagenase solution (1 mg/mL) at 37 °C for 4 h with occasional mixing. The digested dermal mixture was then passed through a 70-µm cell strainer (Becton Dickinson, Heidelberg, Germany) in order to harvest cells. HDFs were cultured in DMEM/F12 supplemented with 10% (*v*/*v*) heat-inactivated fetal calf serum, 1% (*v*/*v*) L-glutamine, and 1% (*v*/*v*) antibiotic-antimycotic solution in a humidified atmosphere (95% air, 5% CO_2) at 37 °C up to passage 5.

Cytotoxicity assay

Potential cytotoxicity of PVP towards HDFs was investigated using a 3-(4,5-dimethyl-2-thiazolyl)-2,5-diphenyltetrazoliumbromide (MTT) colorimetric assay in vitro (Edwards-Gayle et al. 2019). HDFs (10^4 cells/well) were seeded in 96-well plates and permitted to adhere in 100 µL of complete medium at 37 °C for 24 h prior to addition of two-fold serial dilutions of PVP. After 6, 12, and 24 h of cell exposure to the peptide, 15 µL of MTT (5 mg/mL in PBS) was added to each well and permitted to react with the cells for 4 h in dark, followed by removing the supernatant from the wells. Triton X-100 (0.1%; *v*/*v*) was used as a positive control. The formazan crystals were then solubilized by addition of dimethyl sulfoxide (100 µL/well) and the amount of the re-suspended formazan was measured at 570 nm. The percentage of cell survival was calculated using the following equation:

$$\text{Cell survival}(\%) = \left[\frac{(S-B)}{(C-B)}\right] \times 100$$

Where *S*, *C*, and *B* denote the absorbance of the peptide-treated sample, the negative control (no peptide treatment), and the background (MTT solution with DMEM/F12 medium only), respectively.

Morphological observation

After 6, 12, and 24 h of incubation with different concentrations of the peptide, HDFs were visualized by an inverted microscope (Nikon, Eclipse TS100, Tokyo, Japan) to identify the morphological changes as compared to the negative control.

Determination of the selectivity index

As a widely employed parameter, selectivity index (SI) indicates the in vitro specificity of anti-microbials for pathogenic versus eukaryotic cells. The greater the SI, the higher the separation between side effects and desired anti-infective properties. SI was determined in accordance to the following equation (Raja et al. 2017):

$$\text{SI} = \frac{\text{LC}_{50}}{\text{GM}}$$

Where LC_{50} denotes the half lethal concentration of PVP against HDFs after 24 h and GM represents the geometric mean of MIC values from all MRSA strains.

Statistical analysis

All statistical analyses were carried out using SPSS Statistics 20.0 (SPSS Inc. Chicago, Illinois, USA). Quantitative data are expressed as the mean ± standard deviation (SD). The statistical significance of differences between two groups were determined by a *t*-test. *P* values less than 0.05 were considered as statistically significant.

Results

Peptide analysis and synthesis

PVP is a short cationic peptide with a total net charge of + 8. Total hydrophobic ratio and hydrophobic moment of the peptide were 46% and 0.693, respectively. As a tridecapeptide, PVP has a tendency to adopt alpha-helical conformation based upon structural prediction (Fig. 1a). In terms of secondary structure prediction, 9 amino acid residues (69.23%) of PVP take the form of helical structure. The

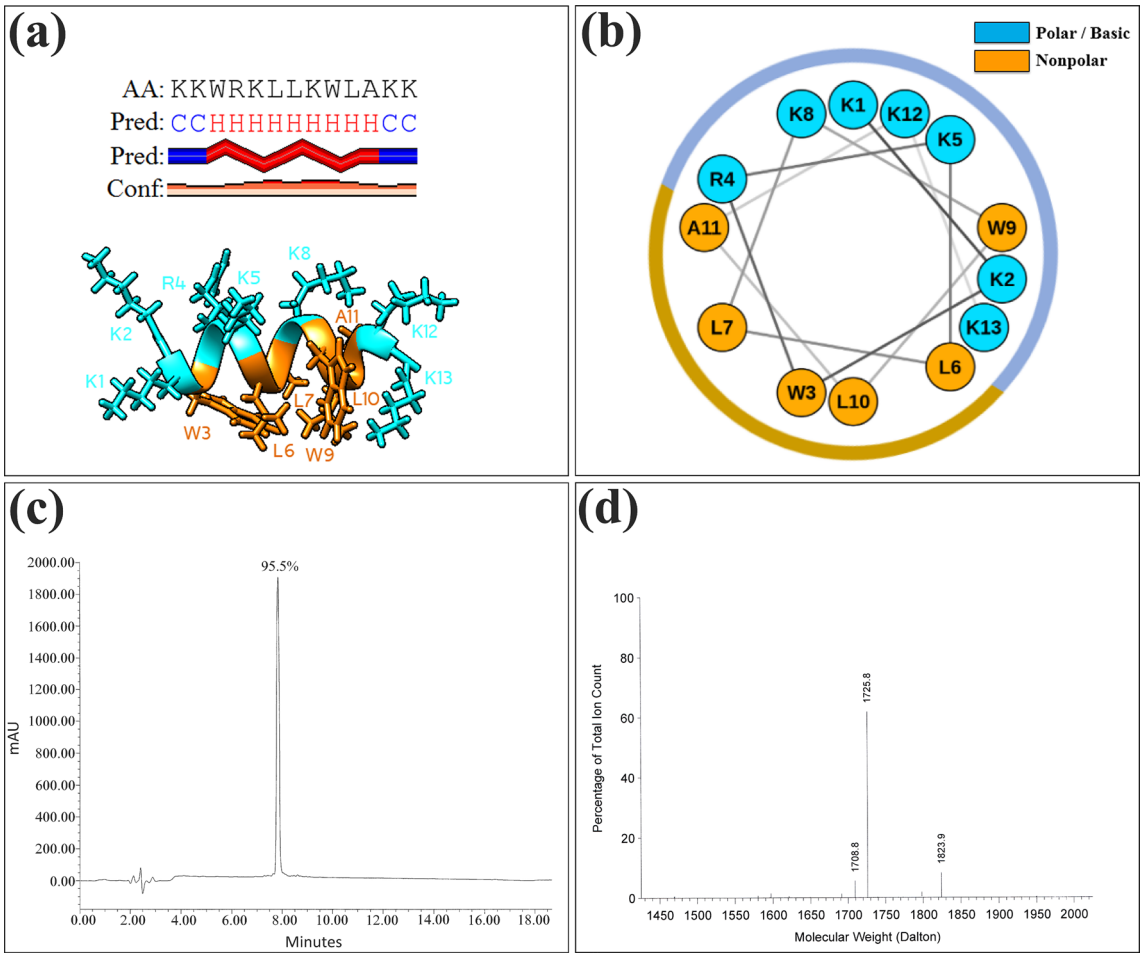

Fig. 1 Predicted secondary (**a**, top) and tertiary structures (**a**, bottom), Schiffer-Edmundson helical wheel diagram (**b**) RP-HPLC chromatogram (**c**), and mass spectrometry data (**d**) of PVP. In panel **a**, AA, Pred, and Conf indicate single-letter amino acid codes, predicted secondary structure (C; random coil, H; helix), and confidence in the prediction, respectively. PVP is also shown in N- to C-terminus direction in panel **a**. Polar/basic and nonpolar amino acid residues are colored light blue and orange, respectively

first I-TASSER model of PVP with high confidence score is shown in Fig. 1a, indicating that the peptide assumes an alpha-helical structure. On the basis of the Schiffer–Edmundson helical wheel diagram (Fig. 1b), the peptide represents an imperfectly amphipathic nature in which hydrophobic and positively charged residues are predominantly clustered on opposing sides of the helical wheel. The purity of PVP was above 95% according to the analytical RP-HPLC chromatogram (Fig. 1c). In addition, the theoretical molecular weight of PVP (1,724.14 Da) was found to be closely similar to its observed molecular weight (1,725.8 Da) obtained from mass spectrometry experiment (Fig. 1d). This suggests that the peptide was correctly synthesized.

Secondary structure analysis of the peptide

The CD spectra of PVP in different environments are depicted in Fig. 2. In deionized water, the CD spectrum of the peptide exhibited a minimum at 198 nm with a shoulder at 220 nm, which is indicative of a predominantly random coil conformation. Addition of up to 50% TFE (*v*/*v*), a lipomimetic solvent, to deionized water resulted in the appearance of two troughs at 222 and 206 nm; this curve profile is characteristic of an alpha-helix structure. The helical content of the peptide was increased from 12% in deionized water to 41% in 50% TFE.

In vitro anti-bacterial assays

S. aureus strains were obtained from ascitic fluid ($n=1$), blood ($n=2$), and wound or tissue ($n=7$). Strains of *S. aureus* having zone of inhibition of ≤ 21 mm to cefoxitin disk (30 µg) were screened as MRSA. In this respect, all of the *S. aureus* strains ($n=10$) were found to be resistant to cefoxitin. Out of these 10 strains, 9 harbored the *mecA* gene using PCR (Table 1).

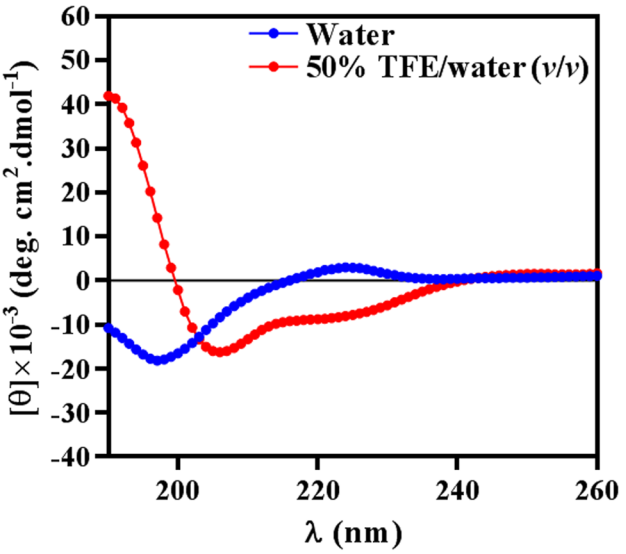

Fig. 2 CD spectra of PVP in deionized water (blue line) and in the presence of 50% (*v*/*v*) TFE (red line)

The in vitro activities of PVP, oxacillin, and vancomycin towards 10 different strains of MRSA are listed in Table 2. All of the anti-bacterial agents were tested at concentrations ranging from 0.25 to 128 µg/mL. MIC and MBC values of PVP against *S. aureus* ATCC 29213 were both equal to 2 µg/mL. The range of MIC values for PVP was 1–16 µg/mL (Fig. 3). Moreover, MIC values of PVP were significantly lower than those of oxacillin ($P = 0.0193$), indicating that the peptide possesses greater anti-bacterial activity against MRSA strains in comparison to oxacillin. However, significant statistical differences were found between MIC values of PVP and vancomycin ($P = 0.0341$), demonstrating that vancomycin has superior anti-bacterial activity against MRSA strains over PVP. Additionally, PVP, oxacillin, and vancomycin had GM values of 4.2, 19.2, and 0.95, respectively. In the majority of cases, the observed MBC values of PVP and antibiotics were equal to or two times the corresponding MIC values. This implies that the peptide and mentioned antibiotics exerted bactericidal effects on tested MRSA strains.

Multistep resistance selection assay

Having shown that PVP exerts potent anti-bacterial effects towards the MRSA strains, we next sought to decipher whether MRSA develop resistance to the peptide. There were no changes in MIC values after consecutive exposures of MRSA to a sub-lethal dose of the peptide (Fig. 4), underlining the fact that PVP did not provoke the development of resistance. Contrarily, there was a one-fold increment in the MIC value of gentamicin after the third passage. Subculturing of MRSA in the presence of ciprofloxacin led to

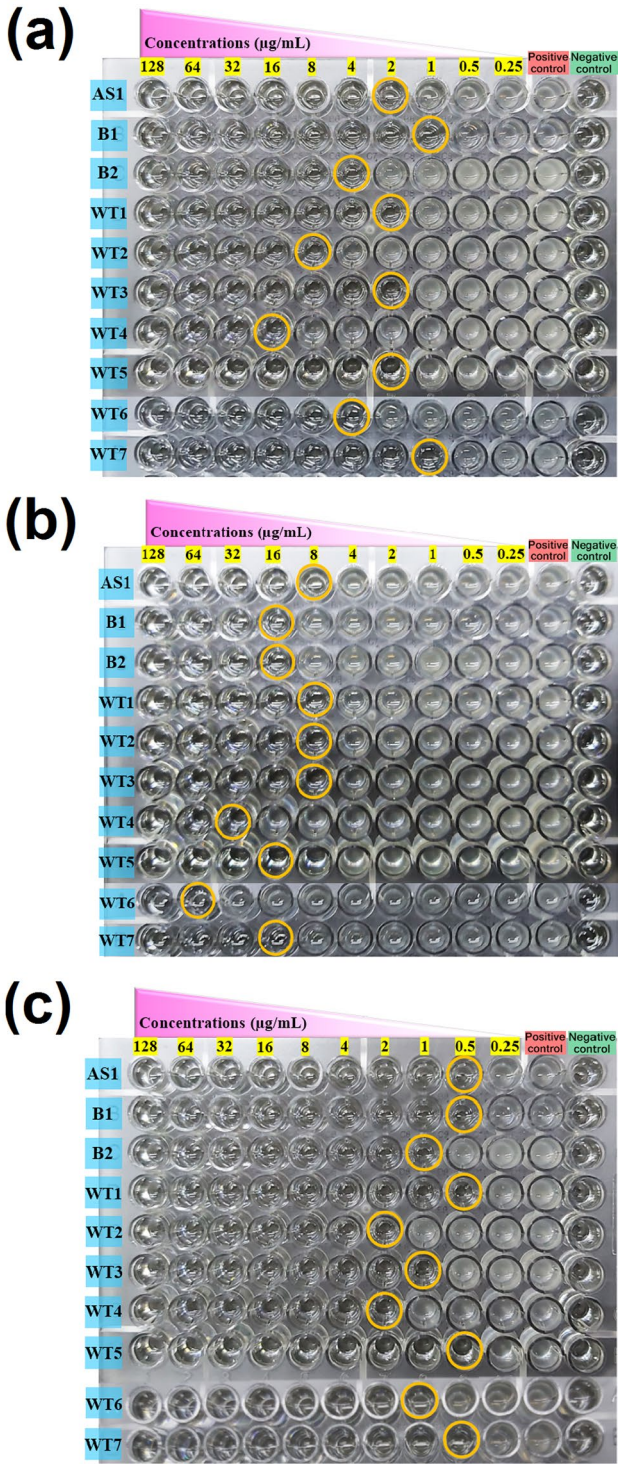

Fig. 3 Broth microdilution assay for MIC determination of anti-bacterial agents against the clinical strains of MRSA. PVP (**a**), oxacillin (**b**), and vancomycin (**c**) were tested at concentrations ranging from 0.25 to 128 µg/mL. For each MRSA strain, positive controls (bacterial inoculation without anti-bacterial agents) and negative controls (MHB only) were also included. Each orange circle denotes the MIC value for the corresponding strain

Table 2 Anti-bacterial activities of PVP, oxacillin, and vancomycin against clinical strains of MRSA

Isolate ID	PVP				Oxacillin				Vancomycin			
	MIC[a]	MBC[b]	R[c]	AI[d]	MIC	MBC	R	AI	MIC	MBC	R	AI
AS1	2	2	1	BC	8	8	1	BC	0.5	0.5	1	BC
B1	1	1	1	BC	16	32	2	BC	0.5	1	2	BC
B2	4	8	2	BC	16	16	1	BC	1	1	1	BC
WT1	2	2	1	BC	8	16	2	BC	0.5	2	4	BS
WT2	8	8	1	BC	8	8	1	BC	2	2	1	BC
WT3	2	2	1	BC	8	32	4	BS	1	1	1	BC
WT4	16	16	1	BC	32	32	1	BC	2	2	1	BC
WT5	2	4	2	BC	16	16	1	BC	0.5	0.5	1	BC
WT6	4	4	1	BC	64	64	1	BC	1	1	1	BC
WT7	1	1	1	BC	16	16	1	BC	0.5	0.5	1	BC

MIC minimum inhibitory concentration (μg/mL), *MBC* minimum bactericidal concentration (μg/mL), *R* MBC/MIC ratio, *AI* Anti-bacterial activity index (*BC* bactericidal, *BS* bacteriostatic)

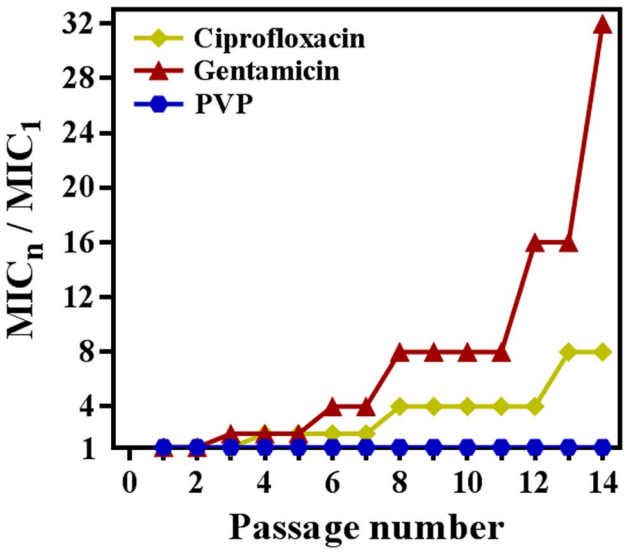

Fig. 4 Multistep resistance selection assay performed on MRSA WT1. Bacterial cells were serially exposed to sub-lethal doses (equivalent to 0.5 × MIC) of PVP (1 μg/mL), ciprofloxacin (0.5 μg/mL), and gentamicin (1 μg/mL) during a fourteen-day-long period. Broth microdilution method was used to evaluate MIC value of the peptide following each consecutive passage

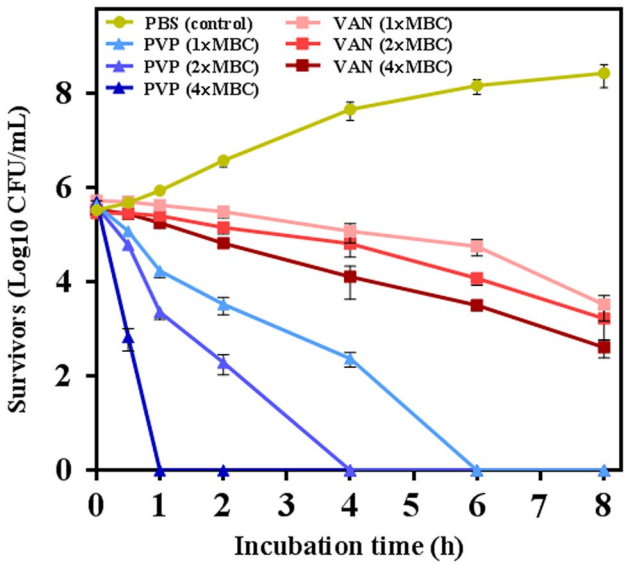

Fig. 5 Kinetics of bacterial killing of PVP against MRSA WT1. Bacterial survival in the presence of MBC and supra-MBC of anti-bacterial agents (PVP and vancomycin) was assessed over a total period of 8 h. Each experiment was carried out at least three times using three replicates. Error bars indicate standard deviations

the onset of resistance as early as passage 4. After 14 passages, 32- and 8-fold increases in MIC values of gentamicin and ciprofloxacin were observed, respectively.

Kinetics of bacterial killing

As evidenced in Fig. 5, PVP reduced viability of bacterial cells in a concentration- and time-dependent fashion. At concentrations equivalent to MBC and supra-MBC, PVP caused a perceptible decrement in MRSA viability only after 30 min of incubation (Fig. 5). Contrary to vancomycin, PVP at 2 × MBC and 4 × MBC required 1 h and 30 min to diminish a $> 3\log_{10}$ of the initial inoculum, respectively. Markedly, 1 h of exposure to 4 × MBC of PVP was sufficient for total bacterial clearance (Fig. 5). However, 4 × MBC of vancomycin failed to wholly wipe out bacterial cells, even after 8 h. These findings suggest that the peptide has faster bactericidal kinetics in comparison to vancomycin.

Cytotoxicity assay

To evaluate if PVP has cell toxicity, HDFs were treated with increasing concentrations of the peptide (0–128 μg/mL) at three different incubation times, as depicted in

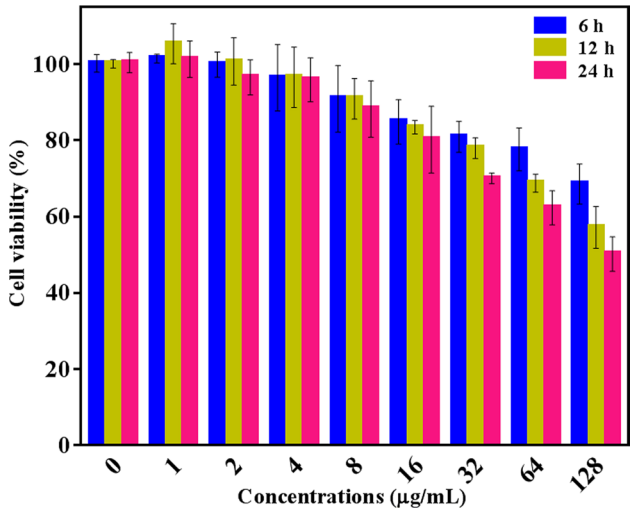

Fig. 6 Cytotoxicity of PVP. Freshly isolated HDFs were incubated with PVP at the indicated concentrations for 6, 12, and 24 h. The cell viability (%) was determined using MTT colorimetric assay. Triton X-100 (0.1%; *v/v*) was employed as a positive control. Three replicates per treatment were performed from three different experiments. The values represent the mean ± standard deviation

Fig. 6. At concentrations below or equal to 4 µg/mL, PVP showed no tangible cytotoxic effects on HDFs. At a concentration of 32 µg/mL, more than 70% of HDFs were still viable even after 24 h of treatment. In addition, LC_{50} value of PVP within 24 h was 128 µg/mL. The peptide decreased viability of HDFs in a concentration- and time-dependent manner (Fig. 6). Treatment of HDFs with Triton X-100 (0.1%; *v/v*) for 6, 12, and 24 h resulted in a complete loss of cell viability.

Morphological observation

The images of HDFs treated with increasing concentrations of PVP are provided in Fig. 7. When compared to the negative controls (without peptide treatment), there were no tangible changes in cell morphology at the peptide concentrations ranging from 1 to 16 µg/mL after 6, 12, and 24 h. The majority of these cells retained their typical fusiform shapes upon microscopic examination. However, distinct morphological changes were discernible in some of the cells exposed to ≥ 32 µg/mL. In this context, some HDFs appeared to be rounded, shrunken, aggregated, and loosely attached to the surface. These findings suggest that the extent of morphological changes of HDFs exposed to PVP were concentration- and time-dependent. In the case of the positive controls (Triton X-100), all of the cells were lysed (Fig. 7).

Determination of the selectivity index

The GM of PVP was 4.2 µg/mL against 10 MRSA strains. As mentioned above, the peptide showed an LC_{50} value of 128 µg/mL. Therefore, SI of PVP was found to be 30.47, indicating greater specificity for bacterial cells compared with HDFs.

Bacterial viability assay

In order to visualize live and damaged MRSA cells by fluorescence microscopy, concurrent staining of bacterial cells with AO and EtBr was employed. In this method, live cells with intact membranes exhibit green fluorescence, while dead cells show orange-red fluorescence. The negative control (PBS-treated) behaved as expected. In light of this, there were no significant changes in color pattern of MRSA cells (Fig. 8a). Exposure of bacterial cells to 1 × MBC and

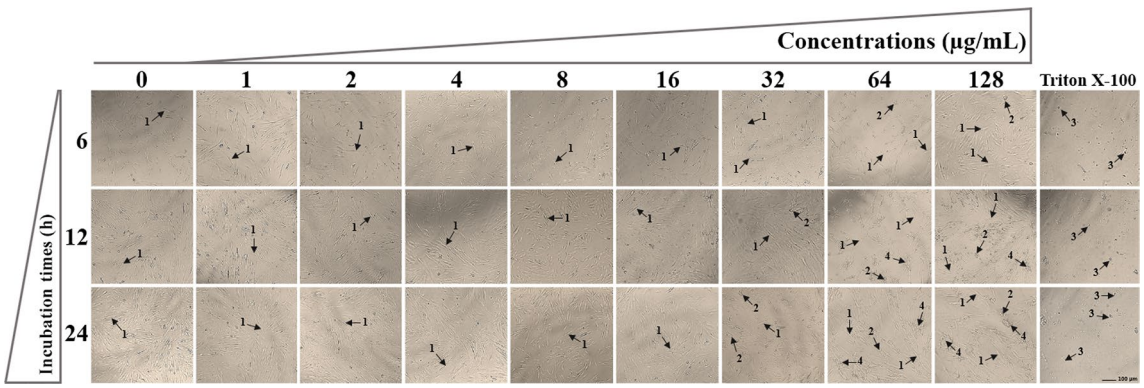

Fig. 7 Morphological changes of HDFs when exposed to various concentrations of PVP (0–128 µg/mL) at three different incubation times (6, 12, and 24 h). The black arrows labeled 1, 2, 3, and 4 represent normal, round-shaped, lysed, and aggregated HDFs, respectively. Triton X-100 (0.1%; *v/v*) was also used as a positive control

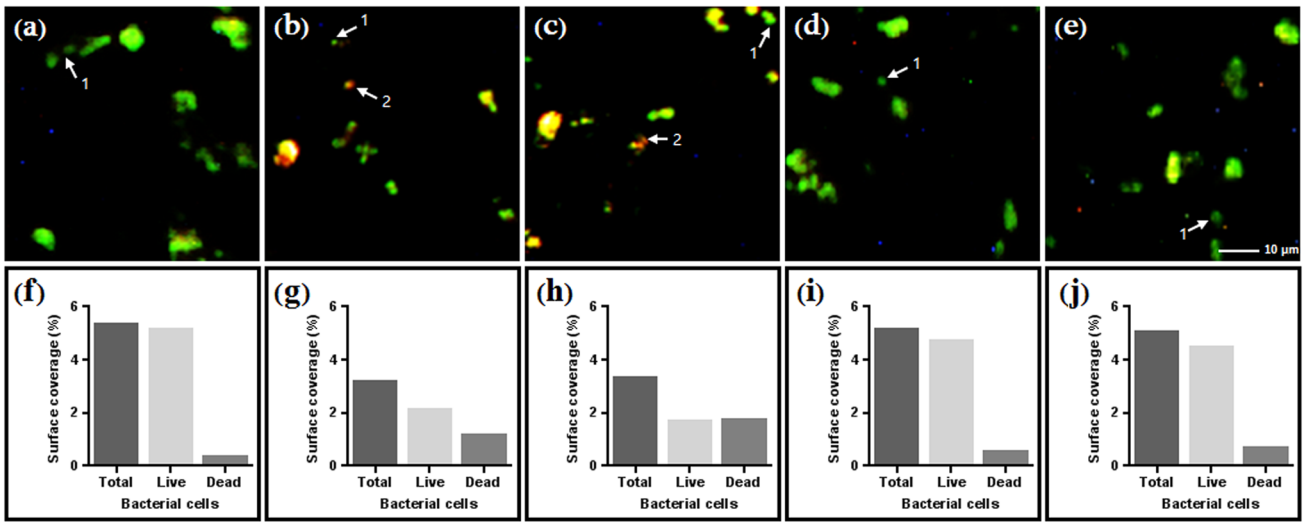

Fig. 8 Fluorescence microscopic images of MRSA WT1 after treatment with the anti-bacterial agents. AO/EtBr double staining method was used for observing live and dead bacteria. PBS-treated bacterial cells were used as a negative control (**a**). Panels **b** (1×MBC, 1 h) and **c** (2×MBC, 1 h) indicate bacterial cells that were exposed to PVP, while panels **d** (1×MBC, 1 h) and **e** (2×MBC, 1 h) represent vancomycin-treated bacterial cells. Furthermore, the white arrows labeled 1 and 2 depict live and dead MRSA cells, respectively. Panels **f** (negative control), **g** (1×MBC of PVP, 1 h), **h** (2×MBC of PVP, 1 h), **i** (1×MBC of vancomycin, 1 h), and **j** (2×MBC of vancomycin, 1 h) represent the percentages of surface areas covered by stained bacteria (i.e. total, live, and dead cells)

2×MBC of PVP for 1 h resulted in enhancement of orange-red fluorescence intensity (Fig. 8b and c). By contrast, no marked changes in orange-red fluorescence intensity of vancomycin-treated-bacterial cells were noted following 1 h of treatment (Fig. 8d and e). As calculated by the ImageJ software, less than 0.25% of the surface area of the negative control image (Fig. 8f) was covered by dead bacterial cells. Noticeably, the percentages of surface areas covered by dead bacterial cells in Fig. 8g and h (PVP-treated MRSA cells) were much higher than those found in Fig. 8i and j (vancomycin-treated MRSA cells). These findings suggest that PVP is superior to vancomycin for killing of MRSA cells after 1 h of incubation.

Membrane permeabilization assay

The membrane-disruptive action of PVP against MRSA was assessed using flow cytometric analysis by measuring the influx of PI into bacterial cells (Fig. 9). As an intercalating DNA-binding dye, PI only enters cells that have damaged membranes. While the PBS-treated MRSA cells (control) displayed negligible PI fluorescence signal (3.12% PI-positive bacteria, Fig. 9a), fluorescence diagram of PVP-treated cells exhibited a marked shift to the right (Fig. 9b and c), implying that PVP has permeabilized bacterial membrane. Noticeably, 24.8% and 41.5% of MRSA cells subjected to 1×MBC and 2×MBC of PVP became permeable for PI after 1 h of incubation. On the contrary, 1 h exposure of MRSA to 1×MBC and 2×MBC of vancomycin resulted in staining of only 4.83% and 7.76% of MRSA cells (Fig. 9d and e), respectively. These observations indicate that vancomycin did not influence the uptake of PI into bacterial cells within 1 h of treatment.

Discussion

The present study was aimed at examining anti-bacterial and cytotoxic effects of the synthetic hybrid peptide PVP. This peptide can be straightforwardly yielded through routine chemical synthesis owing to its short size and amino acid composition. Regarding the latter, a simplified sequence of AMPs like PVP can hasten its translational biomedical applications.

The existence of appropriate amounts of hydrophobic and cationic residues in peptide sequences of short AMPs is a prominent feature which influences their structural properties, potency, and selectivity (Memariani et al. 2017). In the present study, PVP showed a propensity to form an alpha helix based upon structural prediction, which is in line with the behavior of the peptide in a membrane-mimetic environment (50% TFE), as judged by CD spectroscopy. The adoption of this active structure can be attributed to a large percentage of helix-stabilizing residues (e.g. alanine, lysine, and leucine) as well as clustering of hydrophobic amino acids on one face of the helix for insertion into bacterial membrane (Rončević et al. 2019; Wiradharma et al. 2011b). Moreover, cationic amino acid residues such as arginine and lysine may

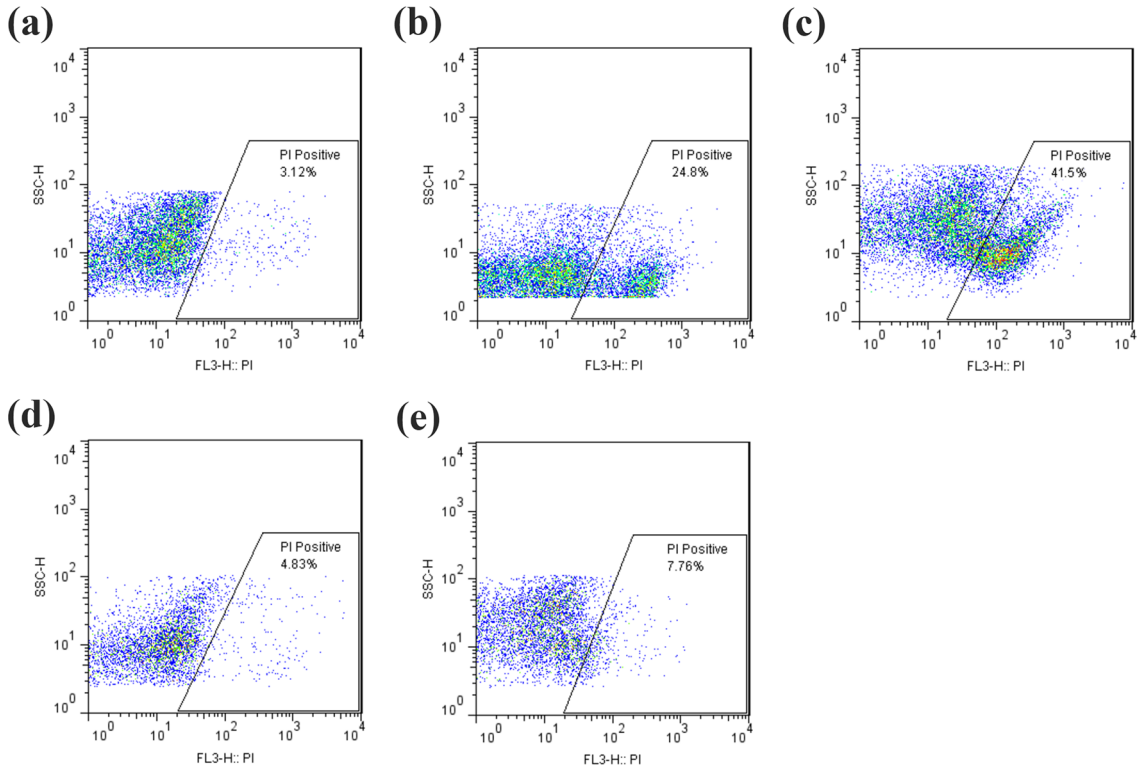

Fig. 9 Flow cytometric analysis by measuring the influx of PI into MRSA WT1. Bacterial cells were treated with PBS (**a**; control), PVP (**b**; 1 × MBC, **c**; 2 × MBC) and vancomycin (**d**; 1 × MBC, **e**; 2 × MBC) for 1 h

facilitate initial electrostatic interaction between PVP and negatively-charged components of bacterial membranes.

In our study, PVP killed the majority of MRSA strains at concentrations lower than or equal to 8 µg/mL, demonstrating its potent bactericidal activity in vitro. During the past years, a great deal of evidence has accrued regarding the ability of short cationic AMPs to inhibit/kill both Gram-positive and Gram-negative bacteria (Kang et al. 2009; Lee et al. 2011; Mohamed et al. 2016; Shin and Hahm 2004; Wiradharma et al. 2011a). For instance, a 13-residue alpha-helical peptide named K_6L_6W (KWKKLLKKLLKLL-NH_2) was shown to exert appreciable anti-bacterial effects (MIC range of 4–8 µM) on laboratory reference strains of bacteria (Shin and Hahm 2004). In one study, Mohamed and co-workers (2016) reported that two short AMPs, WR12 (RWWRWWRRWWRR) and D-IK8 (irikirik), had strong anti-bacterial activities towards all tested multidrug resistant Staphylococcal strains, especially those were resistant to vancomycin and teicoplanin. In an attempt to design and characterize a series of leucine-/lysine-rich AMPs having 5 to 11 residues, Lee et al. (2011) found that $L_5K_2W_2$ (LKWLLKWLL-NH_2) had the most potent anti-bacterial activity with GM values of 1.5 and 5.7 for Gram-positive and Gram-negative bacteria, respectively. In another work, an 11-mer peptide $L_5K_5W_6$ (KKLLKWLKKLL-NH_2) was reported as the most useful peptide among de novo designed AMPs with a short length and a simple amino acid composition since it exhibited not only broad-spectrum anti-bacterial effects but also little hemolytic activity (Kang et al. 2009). Overall, these findings suggest that short AMPs with simplified sequences have the potential to be exploited as a lead compound for designing novel anti-bacterial agents.

A considerable challenge facing anti-microbial agents is induction of microbial drug resistance (Mwangi et al. 2019). Anti-bacterial resistance selection can be assessed through serial passaging of bacteria in the presence of sub-lethal doses of AMPs (Hammer et al. 2012). Herein, we have demonstrated that 14 consecutive cycles of exposure to 0.5 × MIC of PVP did not lead to the development of bacterial resistance to the peptide, which was in sharp contrast to tested antibiotics. Likewise, there have been several examples in the literature regarding the ability of natural or synthetically designed AMPs, but not conventional antibiotics, to inhibit bacterial growth during serial passages without development of peptide-resistant mutants (Mohamed et al. 2014; Myhrman et al. 2013; Wiradharma et al. 2011a). The possible reason behind these observations can arise from the membrane-compromising activity of most cationic AMPs (Diehnelt 2013). It should be hard for bacterial cells to elicit resistance against such AMPs since substantial alteration

in membrane lipid composition would jeopardize bacterial survival (Lohner 2009).

An ideal short AMP should efficiently target microbial pathogens, while not being cytotoxic against human cells. High anti-bacterial activity (i.e. low GM value) in conjugation with low toxicity (i.e. high LC_{50}) is needed for attaining high SI (Raja et al. 2017). In fact, SI provides a beginning point to decide which AMP has adequate therapeutic capacity for further examination in preclinical trials (Memariani et al. 2017). In the present study, PVP showed no or negligible cytotoxicity against HDFs at anti-bacterial concentrations (i.e. ≤ 16 µg/mL). As the peptide concentrations increased to 32 µg/mL or above, however, some HDFs underwent several morphological changes. The SI of PVP was 30.47, suggesting that MRSA can be killed by PVP without inflicting damage upon the host cells. The selective toxicity of cationic AMPs is thought to have arisen from inherent differences in biomembrane lipid compositions of the various cell types (Bobone and Stella 2019). In contrast to eukaryotic cells, Gram-positive bacterial surfaces are rich in phosphatidylglycerol, phosphatidylserine, cardiolipin, and lipoteichoic acid, providing them an overall negative charge. These negatively charged components favor the interaction of bacterial cell membranes with cationic peptides. Other than that, teichoic or teichuronic acids of Gram-positive bacteria confer further negative charges to their bacterial surfaces (Yeaman and Yount 2003). Another difference is the presence of cholesterol inside the eukaryotic membranes that seems to contribute to a weaker hydrophobic interaction between the membrane and the cationic AMPs (Bacalum and Radu 2015). Moreover, it has been proposed that transmembrane potential of prokaryotic cells is typically up to 50% higher than that of most mammalian cells, facilitating selective targeting of bacteria by the cationic peptides (Yeaman and Yount 2003).

In the present study, kinetics of bacterial killing and fluorescence microscopy revealed that PVP dose- and time-dependently diminished the bacterial viability. Notably, PVP exhibited faster rates of bactericidal activity compared to vancomycin. In line with these findings, some studies demonstrated faster bactericidal kinetics of short AMPs in comparison to antibiotics such as vancomycin (Zhang et al. 2019; Mohamed et al. 2016). In addition, fast bactericidal action of PVP supports the findings of flow cytometric analysis in which the peptide showed rapid membrane-permeabilizing activity. It is generally believed that membrane disruption is the main bactericidal mechanism of fast-acting AMPs, particularly at supra-MBC, whereas some AMPs targeting intracellular components (such as proline-rich peptide family) need longer incubation times (typically 6 h ≤) to kill microbial pathogens (Cudic et al. 2002; Memariani and Memariani 2020b). Overall, anti-microbial agents possessing rapid microbicidal activity have several benefits over conventional antibiotics such as restraining the dissemination of bacterial pathogens, improving outcome of the disease, lessening treatment durations, and decreasing the potential development of microbial resistance (Alder and Eisenstein 2004).

Conclusions

The growing problem of anti-microbial resistance among bacterial pathogens necessitates the discovery and development of novel anti-microbial substances. As a short AMP with a helix-forming propensity, PVP was found to be efficient in eradication of MRSA strains in vitro. The peptide not only exerts potent bactericidal effects, but it also possesses negligible cytotoxicity against HDFs. It seems that membrane permeabilization is the main mechanism of action by which PVP kills MRSA. In addition, PVP did not provoke the development of bacterial resistance during serial passages. Though the results reported herein reflect the in vitro effectiveness of PVP, in vivo activities of the peptide should be further evaluated to better understand its possible therapeutic effects.

Acknowledgements The present study was supported by funds from Skin Research Center, Shahid Beheshti University of Medical Sciences, Tehran, Iran. Authors would like to thank Maryam Ghodrati for her expert technical assistance.

Authors' contributions HM and MM jointly contributed to all phases of this study (conception, experimental design, data analysis, practical work, and authorship of the manuscript). ZB and FA partially participated in practical work. HMO, RMR, and SN critically reviewed and edited the manuscript. All authors read and approved the final manuscript.

Compliance with ethical standards

Conflict of interest The authors declare that they have no competing interests.

Ethical approval All of the procedures was approved by the Ethical Committee of Shahid Beheshti University of Medical Sciences, Tehran, Iran (Ethics code: IR. SBMU.REC.1398.008) and was carried out in accordance with the principles of the Declaration of Helsinki.

References

Alder J, Eisenstein B (2004) The advantage of bactericidal drugs in the treatment of infection. Curr Infect Dis Rep 6:251–253. https://doi.org/10.1007/s11908-004-0042-1

Bacalum M, Radu M (2015) Cationic antimicrobial peptides cytotoxicity on mammalian cells: an analysis using therapeutic Index integrative concept. Int J Pept Res Ther 21:47–55. https://doi.org/10.1007/s10989-014-9430-z

Baskić D, Popović S, Ristić P, Arsenijević NN (2006) Analysis of cycloheximide-induced apoptosis in human leukocytes: fluorescence microscopy using annexin V/propidium iodide versus acridin orange/ethidium bromide. Cell Biol Int 30(11):924–932. https://doi.org/10.1016/j.cellbi.2006.06.016

Bobone S, Stella L (2019) Selectivity of antimicrobial peptides: a complex interplay of multiple equilibria. in antimicrobial peptides: basics for clinical application; Matsuzaki K, Ed. Springer Singapore: Singapore:175–214. https://doi.org/10.1007/978-981-13-3588-4_11

Boutiba-Ben Boubaker I, Ben Abbes R, Ben Abdallah H, Mamlouk K, Mahjoubi F, Kammoun A, Hammami A, Ben Redjeb S (2004) Evaluation of a cefoxitin disk diffusion test for the routine detection of methicillin-resistant *Staphylococcus aureus*. Clin Microbiol Infect 10:762–765. https://doi.org/10.1111/j.1469-0691.2004.00919.x

Brand GD, Ramada MHS, Manickchand JR, Correa R, Ribeiro DJS, Santos MA, Vasconcelos AG, Abrão FY, Prates MV, Murad AM, Cardozo Fh JL, Leite JRSA, Magalhães KG, Oliveira AL, Bloch C Jr (2019) Intragenic antimicrobial peptides (IAPs) from human proteins with potent antimicrobial and anti-inflammatory activity. PLoS One 14(8):e0220656. https://doi.org/10.1371/journal.pone.0220656

CDC (2019) Antibiotic Resistance Threats in the United States. Atlanta, GA: U.S. Department of Health and Human Services. https://doi.org/10.15620/cdc:82532

Chatterjee A, Rai S, Guddattu V, Mukhopadhyay C, Saravu K (2018) Is methicillin-resistant *Staphylococcus aureus* infection associated with higher mortality and morbidity in hospitalized patients? A cohort study of 551 patients from South Western India. Risk Manag Healthc Policy 11:243–250. https://doi.org/10.2147/RMHP.S176517

CLSI (2019) M100 Performance Standards for Antimicrobial Susceptibility Testing, 29th edn. Clinical and Laboratory Standards Institute, Wayne

Cudic M, Condie BA, Weiner DJ, Lysenko ES, Xiang ZQ, Insug O, Bulet P, Otvos LJr (2002) Development of novel antibacterial peptides that kill resistant isolates. Peptides 23(12):2071–2083. https://doi.org/10.1016/s0196-9781(02)00244-9

Diehnelt CW (2013) Peptide array based discovery of synthetic antimicrobial peptides. Front Microbiol 4:402. https://doi.org/10.3389/fmicb.2013.00402

Edwards-Gayle CJC, Castelletto V, Hamley IW, Barrett G, Greco F, Hermida-Merino D, Rambo RP, Seitsonen J, Ruokolainen J (2019) Self-assembly, antimicrobial activity, and membrane interactions of arginine-capped peptide bola-amphiphiles. ACS Appl Bio Mater 2(5):2208–2218. https://doi.org/10.1021/acsabm.9b00172

Gould IM, David MZ, Esposito S, Garau J, Lina G, Mazzei T, Peters G (2012) New insights into meticillin-resistant *Staphylococcus aureus* (MRSA) pathogenesis, treatment and resistance. Int J Antimicrob Agents 39(2):96–104. https://doi.org/10.1016/j.ijantimicag.2011.09.028

Guinoiseau E, Luciani A, Rossi PG, Quilichini Y, Ternengo S, Bradesi P, Berti L (2010) Cellular effects induced by *Inula graveolens* and *Santolina corsica* essential oils on *Staphylococcus aureus*. Eur J Clin Microbiol Infect Dis 29(7):873–879. https://doi.org/10.1007/s10096-010-0943-x

Hammer KA, Carson CF, Riley TV (2012) Effects of *Melaleuca alternifolia* (tea tree) essential oil and the major monoterpene component terpinen-4-ol on the development of single- and multistep antibiotic resistance and antimicrobial susceptibility. Antimicrob Agents Chemother 56(2):909–915. https://doi.org/10.1128/AAC.05741-11

Haney EF, Straus SK, Hancock REW (2019) Reassessing the host defense peptide landscape. Front Chem 7:43. https://doi.org/10.3389/fchem.2019.00043

Hotchkiss RS, Opal SM (2020) Activating immunity to fight a foe – a new path. N Engl J Med 382(13):1270–1272. https://doi.org/10.1056/NEJMcibr1917242

Jeyanthi V, Velusamy P (2016) Anti-methicillin resistant *Staphylococcus aureus* compound isolation from halophilic *Bacillus amyloliquefaciens* MHB1 and determination of its mode of action using electron microscope and flow cytometry analysis. Indian J Microbiol 56(2):148–157. https://doi.org/10.1007/s12088-016-0566-8

Kang SJ, Won HS, Choi WS, Lee BJ (2009) *De novo* generation of antimicrobial LK peptides with a single tryptophan at the critical amphipathic interface. J Pept Sci 15(9):583–588. https://doi.org/10.1002/psc.1149

Kluytmans J, Harbarth S (2020) MRSA transmission in the community: emerging from under the radar. Lancet Infect Dis 20(2):147–149. https://doi.org/10.1016/S1473-3099(19)30539-0

Konaté K, Mavoungou JF, Lepengué AN, Aworet-Samseny RR, Hilou A, Souza A, Dicko MH, M'batchi B (2012) Antibacterial activity against β-lactamase producing methicillin and ampicillin-resistants *Staphylococcus aureus*: fractional inhibitory concentration index (FICI) determination. Ann Clin Microbiol Antimicrob 11:18. https://doi.org/10.1186/1476-0711-11-18

Koo HB, Seo J (2019) Antimicrobial peptides under clinical investigation. Pept Sci 111(5):e24122. https://doi.org/10.1002/pep2.24122

Lazzaro BP, Zasloff M, Rolff J (2020) Antimicrobial peptides: application informed by evolution. Science 368(6490):eaau5480. https://doi.org/10.1126/science.aau5480

Lee DL, Mant CT, Hodges RS (2003) A novel method to measure self-association of small amphipathic molecules: temperature profiling in reversed-phase chromatography. J Biol Chem 278(25):22918–22927. https://doi.org/10.1074/jbc.M301777200

Lee SH, Kim SJ, Lee YS, Song MD, Kim IH, Won HS (2011) *De novo* generation of short antimicrobial peptides with simple amino acid composition. Regul Pept 166(1–3):36–41. https://doi.org/10.1016/j.regpep.2010.08.010

Lohner K (2009) New strategies for novel antibiotics: peptides targeting bacterial cell membranes. Gen Physiol Biophys 28:105–116. https://doi.org/10.4149/gpb_2009_02_105

Memariani H, Shahbazzadeh D, Ranjbar R, Behdani M, Memariani M, Bagheri KP (2017) Design and characterization of short hybrid antimicrobial peptides From pEM-2, mastoparan-VT1, and mastoparan-B. Chem Biol Drug Des 89(3):327–338. https://doi.org/10.1111/cbdd.12864

Memariani H, Shahbazzadeh D, Sabatier JM, Pooshang Bagheri K (2018) Membrane-active peptide PV3 efficiently eradicates multidrug-resistant *Pseudomonas aeruginosa* in a mouse model of burn infection. APMIS 126(2):114–122. https://doi.org/10.1111/apm.12791

Memariani H, Memariani M (2020a) Therapeutic and prophylactic potential of anti-microbial peptides against coronaviruses. Ir J Med Sci. https://doi.org/10.1007/s11845-020-02232-4

Memariani H, Memariani M (2020b) Anti-fungal properties and mechanisms of melittin. Appl Microbiol Biotechnol. https://doi.org/10.1007/s00253-020-10701-0

Mikut R, Ruden S, Reischl M, Breitling F, Volkmer R, Hilpert K (2016) Improving short antimicrobial peptides despite elusive rules for activity. Biochim Biophys Acta 1858(5):1024–1033. https://doi.org/10.1016/j.bbamem.2015.12.013

Mishra B, Lushnikova T, Golla RM, Wang X, Wang G (2017) Design and surface immobilization of short anti-biofilm peptides. Acta Biomater 49:316–328. https://doi.org/10.1016/j.actbio.2016.11.061

Mohamed MF, Hammac GK, Guptill L, Seleem MN (2014) Antibacterial activity of novel cationic peptides against clinical isolates of multidrug resistant *Staphylococcus pseudintermedius* from infected dogs. PLoS ONE 9(12):e116259. https://doi.org/10.1371/journal.pone.0116259

Mohamed MF, Abdelkhalek A, Seleem MN (2016) Evaluation of short synthetic antimicrobial peptides for treatment of drug-resistant and intracellular *Staphylococcus aureus*. Sci Rep 6:29707. https://doi.org/10.1038/srep29707

Mookherjee N, Anderson MA, Haagsman HP, Davidson DJ (2020) Antimicrobial host defence peptides: functions and clinical potential. Nat Rev Drug Discov 19(5):311–332. https://doi.org/10.1038/s41573-019-0058-8

Moravvej H, Abdollahimajd F, Naseh MH, Piravar Z, Abolhasani E, Mozafari N, Niknejad H (2018) Cultured allogeneic fibroblast injection vs. fibroblasts cultured on amniotic membrane scaffold for dystrophic epidermolysis bullosa treatment. Br J Dermatol 179(1):72–79. https://doi.org/10.1111/bjd.16338

Moravvej H, Memariani M, Memariani H, Robati RM, Gheisari M (2020) Can antimicrobial peptides be repurposed as a novel therapy for keloids? Dermatology. https://doi.org/10.1159/000506831

Morelli JJ, Hogan PG, Sullivan ML, Muenks CE, Wang JW, Thompson RM, Burnham CA, Fritz SA (2015) Antimicrobial susceptibility profiles of *Staphylococcus aureus* isolates recovered from humans, environmental surfaces, and companion animals in households of children with community-onset methicillin-resistant *S. aureus* infections. Antimicrob Agents Chemother 59(10):6634–6637. https://doi.org/10.1128/AAC.01492-15

Murakami K, Minamide W, Wada K, Nakamura E, Teraoka H, Watanabe S (1991) Identification of methicillin-resistant strains of *Staphylococci* by polymerase chain reaction. J Clin Microbiol 29(10):2240–2244

Mwangi J, Yin Y, Wang J, Yang M, Li Y, Zhang Z, Lai R (2019) The antimicrobial peptide ZY4 combats multidrug-resistant *Pseudomonas aeruginosa* and *Acinetobacter baumannii* infection. Proc Natl Acad Sci USA 116(52):26516–26522. https://doi.org/10.1073/pnas.1909585117

Myhrman E, Håkansson J, Lindgren K, Björn C, Sjöstrand V, Mahlapuu M (2013) The novel antimicrobial peptide PXL150 in the local treatment of skin and soft tissue infections. Appl Microbiol Biotechnol 97:3085–3096. https://doi.org/10.1007/s00253-012-4439-8

Ong ZY, Wiradharma N, Yang YY (2014) Strategies employed in the design and optimization of synthetic antimicrobial peptide amphiphiles with enhanced therapeutic potentials. Adv Drug Deliv Rev 78:28–45. https://doi.org/10.1016/j.addr.2014.10.013

Rahnamaeian M, Vilcinskas A (2015) Short antimicrobial peptides as cosmetic ingredients to deter dermatological pathogens. Appl Microbiol Biotechnol 99(21):8847–8855. https://doi.org/10.1007/s00253-015-6926-1

Raja Z, André S, Abbassi F, Humblot V, Lequin O, Bouceba T, Correia I, Casale S, Foulon T, Sereno D, Oury B, Ladram A (2017) Insight into the mechanism of action of temporin-SHa, a new broad-spectrum antiparasitic and antibacterial agent. PLoS ONE 12(3):e0174024. https://doi.org/10.1371/journal.pone.0174024

Reuter M, Kruger DH (2020) Approaches to optimize therapeutic bacteriophage and bacteriophage-derived products to combat bacterial infections. Virus Genes 56:136–149. https://doi.org/10.1007/s11262-020-01735-7

Rončević T, Puizina J, Tossi A (2019) Antimicrobial peptides as anti-infective agents in pre-post-antibiotic era? Int J Mol Sci 20:5713. https://doi.org/10.3390/ijms20225713

Schiffer M, Edmundson AB (1967) Use of helical wheels to represent the structures of proteins and to identify segments with helical potential. Biophys J 7(2):121–135. https://doi.org/10.1016/S0006-3495(67)86579-2

Shagaghi N, Palombo EA, Clayton AHA, Bhave M (2018) Antimicrobial peptides: biochemical determinants of activity and biophysical techniques of elucidating their functionality. World J Microbiol Biotechnol 34(4):62. https://doi.org/10.1007/s11274-018-2444-5

Shin SY, Hahm KA (2004) Short α-helical antimicrobial peptide with antibacterial selectivity. Biotechnol Lett 26:735–739. https://doi.org/10.1023/B:BILE.0000024098.83025.de

Smart SS, Mason TJ, Bennell PS, Maeij NJ, Geysen HM (1996) High-throughput purity estimation and characterisation of synthetic peptides by electrospray mass spectrometry. Int J Pept Protein Res 47:47–55. https://doi.org/10.1111/j.1399-3011.1996.tb00809.x

Tille PM (2017) Bailey & Scott's diagnostic microbiology, 14th edn. Elsevier, St. Louis

Wang C, Yang C, Chen YC, Ma L, Huang K (2019) Rational design of hybrid peptides: a novel drug design approach. Curr Med Sci 39(3):349–355. https://doi.org/10.1007/s11596-019-2042-2

Wibowo D, Zhao CX (2019) Recent achievements and perspectives for large-scale recombinant production of antimicrobial peptides. Appl Microbiol Biotechnol 103(2):659–671. https://doi.org/10.1007/s00253-018-9524-1

Wiradharma N, Khan M, Yong LK, Hauser CAE, Seow SV, Zhang S, Yang YY (2011a) The effect of thiol functional group incorporation into cationic helical peptides on antimicrobial activities and spectra. Biomaterials 32(34):9100–9108. https://doi.org/10.1016/j.biomaterials.2011.08.020

Wiradharma N, Khoe U, Hauser CAE, Seow SV, Zhang S, Yang YY (2011b) Synthetic cationic amphiphilic α-helical peptides as antimicrobial agents. Biomaterials 32(8):2204–2212. https://doi.org/10.1016/j.biomaterials.2010.11.054

Yeaman MR, Yount NY (2003) Mechanisms of antimicrobial peptide action and resistance. Pharmacol Rev 55:27–55. https://doi.org/10.1124/pr.55.1.2

Zhang Y, Teng D, Mao R, Wang X, Xi D, Hu X, Wang J (2014) High expression of a plectasin-derived peptide NZ2114 in *Pichia pastoris* and its pharmacodynamics, postantibiotic and synergy against *Staphylococcus aureus*. Appl Microbiol Biotechnol 98(2):681–694. https://doi.org/10.1007/s00253-013-4881-2

Zhang R, Wang Z, Tian Y, Yin Q, Cheng X, Lian M, Zhou B, Zhang X, Yang L (2019) Efficacy of antimicrobial peptide DP7, designed by machine-learning method, against methicillin-resistant *Staphylococcus aureus*. Front Microbiol 10:1175. https://doi.org/10.3389/fmicb.2019.01175